Characterization of the first High-Z AGIPD detector prototypes

Oleksandr Koretskyi, National University of Kyiv-Mohyla Academy, Ukraine

September 5, 2024

Abstract

This report presents the characterization of the first high-Z AGIPD detector prototypes. The study is part of a broader effort to overcome the limitations of traditional silicon-based detectors, particularly at higher photon energies. To address these challenges, detectors with sensors made from high-Z materials, such as cadmium zinc telluride (CdZnTe), cadmium telluride (CdTe), and gallium arsenide (GaAs), were considered as a solution. The characterization was performed with the first module, composed of a CdZnTe quad sensor, which underwent detailed evaluations. The experiments involved measuring the sensor's response under varying voltage conditions, assessing leakage current, and conducting pulse capacitor scans to evaluate the ASIC response and configurations. Additionally, the sensor was tested using an X-ray source to evaluate its behavior under active radiation exposure. During these tests, the sensor's response to varying voltages was recorded, and characteristic curves were generated for a region of interest within the beam image. The results showed a higher-than-expected leakage current, suggesting further investigation is needed into the sensor material and configuration. Gain threshold settings and switching behavior also revealed the need for optimization to ensure accurate calibration and reliable performance. Planned beamtime at the High Energy Density (HED) facility in November 2024 will be essential in characterizing the sensor's afterglow behavior and its response to high-flux X-ray conditions. These results will provide valuable insights into the viability of high-Z AGIPD detectors for applications in high-energy X-ray experiments.

Contents

1 Introduction

X-ray detection plays a pivotal role in various scientific disciplines, including medical imaging, material science, photon science and high-energy physics experiments. The performance of X-ray detectors is highly dependent on the materials used in their construction. While silicon is widely used due to its maturity and robust performance in many applications, its lower efficiency in detecting high-energy X-rays poses limitations.

To address these challenges, the development of high-Z (high atomic number) material detectors has gained significant attention. High-Z materials such as germanium (Ge), gallium arsenide (GaAs), cadmium telluride (CdTe), and cadmium zinc telluride (CZT) exhibit higher absorption efficiencies for high-energy X-rays compared to silicon, making them ideal candidates for advanced X-ray detection systems.

In the context of this research, the Adaptive Gain Integrating Pixel Detector (AGIPD), originally designed for the European XFEL, presents a unique opportunity to evaluate the performance of high-Z materials under such a challenging X-ray intensity. The AGIPD detector is equipped to handle XFEL's demanding pulse repetition rates, which emit up to 27,000 pulses per second. However, the limitations of silicon sensors at the higher photon energy ranges of 20-30 keV, desired by some of the Eu.XFEL instruments like the High Energy Density (HED) facility, have prompted the development of AGIPD modules compatible with high-Z materials.

These detectors will be tested at HED, with experiments scheduled for November 2024. The outcomes of these tests will provide critical insights into the viability of high-Z AGIPD detectors for future high-energy X-ray applications.

2 Theory

2.1 Hybrid Pixel Detectors

Pixel detectors are widely used in scientific research for their ability to provide high spatial resolution and efficient signal processing in detecting charged particles or photons. These detectors consist of an array of individual pixels, each acting as an independent detector, which enables precise localization of particle interactions. The hybrid nature of pixel detectors, where the sensor and readout electronics are separate but closely integrated, enhances their versatility and performance in a wide range of applications.

Figure 1 illustrates the concept and assembly of the AGIPD detector. The sensor is connected to a readout pixel array via bump bonds.

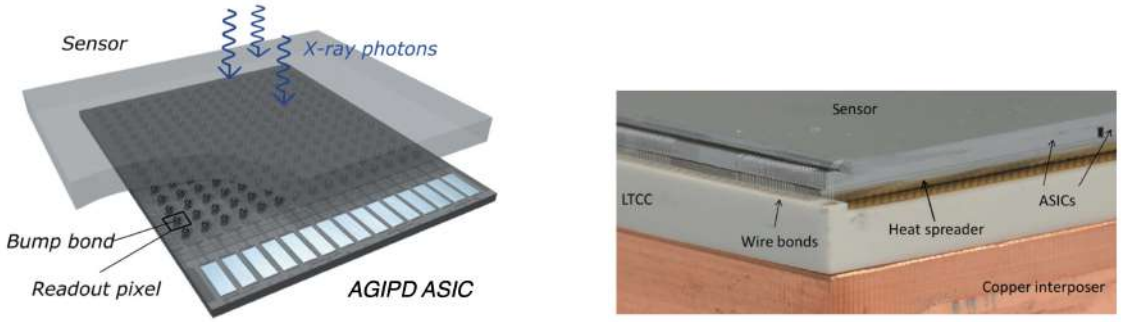

(a) Conceptual design of a hybrid pixel array detector

(b) Macro photograph of the edge of the module

Figure 1: Construction of a hybrid pixel detector

One essential feature of hybrid pixel detectors is their ability to operate with the sensor and readout electronics (the ASIC) as two separate layers. This design allows for independent optimization of both layers, which is critical in high-performance detectors like AGIPD. The connection between the sensor and the readout pixel array is established through bump bonds, which are microscopic metal contacts. These bonds provide a fast signal connection, enabling the efficient transfer of charge collected by the sensor to the readout electronics. Each pixel in the sensor is uniquely connected to a corresponding pixel in the readout layer. This individual pixel-to-pixel interaction ensures precise spatial resolution and efficient signal processing, making hybrid pixel detectors ideal for high-speed and high-flux environments, such as those encountered in XFEL experiments.

2.2 Semiconductor sensors

A semiconductor sensor works by detecting charged particles or photons through the creation of electron-hole pairs within the semiconductor. When these particles interact with the semiconductor, they ionize the atoms, generating electron-hole pairs. The energy required to create these pairs is determined by the material's bandgap, which is the energy difference between the valence and conduction bands. If the energy of the incoming photon or particle is greater than the bandgap, it excites electrons into the conduction band, leaving behind holes in the valence band. These pairs are separated by an electric field in the reverse-biased p-n junction, with electrons drifting toward

the positive electrode and holes toward the negative electrode. The drift velocity v of the carriers is given by:

$$v = \mu \cdot E$$

where μ is the mobility of the carriers and E is the electric field.

By calculating the depletion zone width using the provided equation, we can estimate the minimum thickness required for the sensor to achieve full charge collection and efficient detection. Conversely, the equation can also be used to calculate the ideal bias voltage needed to fully deplete a given sensor thickness.

The width of the depletion zone W is given by:

$$W = \sqrt{\frac{2\epsilon_s(V + V_{\text{bi}})}{e \cdot N_{\text{eff}}}}$$

where ϵ_s is the permittivity of the material, V_{bi} is the built-in potential, V is the applied bias voltage and N_{eff} is the effective doping concentration.

These processes convert the physical interaction of particles with the silicon into an electrical signal, which is then measured and analysed.

2.2.1 High-Z sensors

Silicon has been the most commonly used semiconductor material due to its maturity and robustness, but it has limitations, especially in detecting high-energy X-rays. This limitation has led to the development and increasing use of high-Z (high atomic number) semiconductors, which are better suited for high-energy X-ray applications. High-Z materials, such as germanium (Ge), gallium arsenide (GaAs), cadmium telluride (CdTe), and cadmium zinc telluride (CZT), offer higher X-ray absorption efficiency, making them ideal for applications in a higher energy range.

Germanium is one of the most mature high-Z semiconductors, widely used in X-ray detectors. It offers excellent energy resolution and high efficiency for detecting hard X-rays. However, due to its relatively low bandgap (0.7 eV), germanium detectors need to be cooled to minimize leakage current and consequently noise. Gallium Arsenide is known for its stability, making it a strong candidate for imaging detectors. It is less suited for spectroscopic applications due to its poorer energy resolution compared to germanium. Cadmium Telluride (CdTe) and Cadmium Zinc Telluride (CZT) both are compound semiconductors that offer high detection efficiency at extreme X-ray energies. CdTe, in particular, is valued for its short X-ray attenuation lengths, which make it suitable for applications requiring thin sensors. CZT provides the added benefit of a wider bandgap, resulting in lower leakage current and improved performance at room temperature.

The graph (Figure 2) shows the photoelectric absorption of different semiconductor materials — silicon (Si), gallium arsenide (GaAs), germanium (Ge), and cadmium telluride (CdTe) — as a function of X-ray energy (keV). Each material's curve represents its efficiency in absorbing X-rays across a range of energies. CdTe (1000 µm) demonstrates the highest absorption efficiency over a wide energy range, making it suitable for high-energy applications. Silicon (500 µm), on the other hand, loses absorption efficiency rapidly beyond 20 keV, highlighting its limitation at higher photon energies.

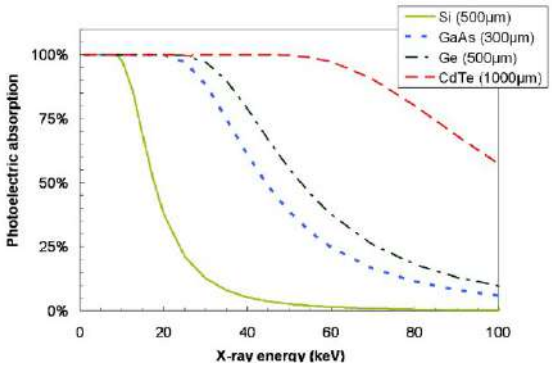

Figure 2: Photoelectric absorption depending on the sensor material

2.3 The AGIPD Detector

The Adaptive Gain Integrating Pixel Detector (AGIPD) was specifically developed to meet the unique requirements of the European X-Ray Free Electron Laser (XFEL), which is a cutting-edge facility delivering ultra-short, intense, and coherent X-ray pulses. The European XFEL has a distinctive pulse repetition pattern, where X-ray pulses are emitted in bursts or "pulse trains" with an intra-train repetition rate as high as 4.5 MHz. Each pulse train contains up to 2,700 pulses, resulting in a total of up to 27,000 pulses per second.

AGIPD is a hybrid pixel detector designed to cope with these challenging conditions. The readout chip, or Application Specific Integrated Circuit (ASIC), is bump-bonded to the sensor, forming the heart of the detection system.

AGIPD serves as the primary detector for the High Energy Density (HED) instrument. However, at HED's photon energy range of 20-30 keV, the current AGIPD "mini-Half" detector (Figure 3 a), which is bonded to a 500 µm thick silicon sensor, suffers from reduced quantum efficiency and potential damage to the underlying ASICs.

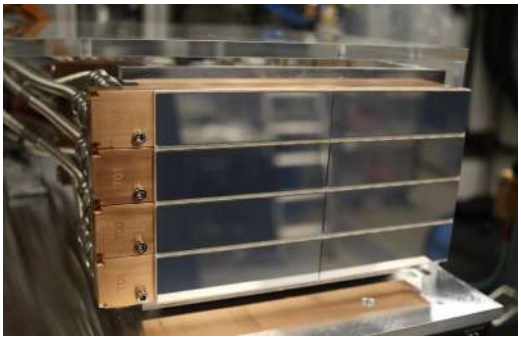

(a) AGIPD mini-Half with silicon sensor

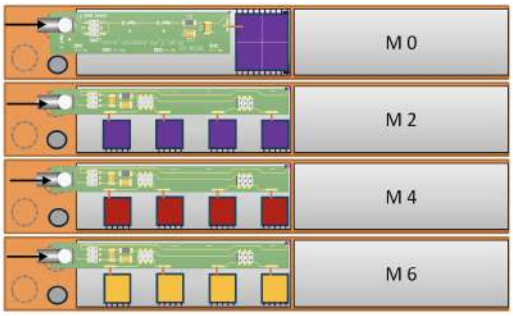

(b) Prototype test model (purple - CdZnTe; red - CdTe; yellow - GaAs)

Figure 3: AGIPD mini-Half

To operate within the same energy range, a decision was made to utilize sensors made from

high-Z materials instead of traditional silicon sensors. As part of this initiative, it was decided to develop a prototype test module (Figure 3 b), which will undergo testing at the High Energy Density (HED) facility, scheduled for November 2024. The primary focus of this testing will be to characterize two key aspects of the sensors: afterglow effects and their response under high-flux conditions.

2.3.1 ecAGIPD

AGIPD uses a hole-collecting mechanism in its standard silicon sensor design. In this setup, when X-rays hit the sensor, electron-hole pairs are generated. Holes are collected at the electrodes, a process typically slower than electron collection. ecAGIPD, as the name suggests, uses an electron-collecting mechanism, which is generally faster and more efficient. In an electron-collecting setup, electrons, being lighter and more mobile than holes, are collected at the electrodes. This leads to faster signal processing and better performance in high-rate environments, specially for compound semiconductor sensors, which can suffer from defects and consequently trapping. During our research we worked with ecAGIPD.

3 Methodology

To model the test prototype for the High Energy Density (HED) facility (Figure 3 b), a decision was made to first evaluate individual modules equipped with sensors made from different high-Z materials. The sensor materials selected for testing include CdZnTe with a thickness of 2 mm, in both single and quad (2x2) shapes, GaAs with a thickness of 500 µm in single sensor shapes, and CdTe with a thickness of 1 mm in single shapes (Figure 4). These sensors will be tested individually, and once the performance of each material is characterized, they are planned to be assembled together for comprehensive testing.

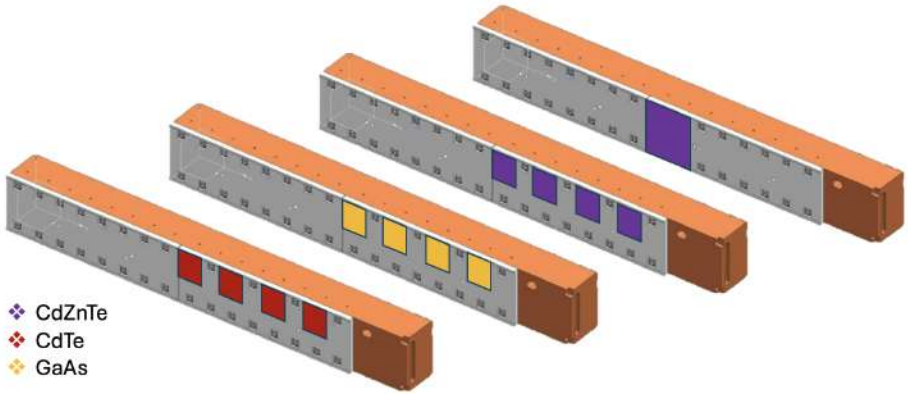

Figure 4: Modules for the final test prototype

This structured approach allows us to assess the capabilities of each sensor material independently, ensuring that we capture the unique properties and performance characteristics of CdZnTe, GaAs, and CdTe. Ultimately, the goal is to determine the most suitable material for high-energy

X-ray applications, such as those required at the HED facility, while ensuring reliable data collection and sensor durability under extreme conditions.

During the course of our work, we focused on conducting detailed measurements for the CdZnTe quad sensor. As a result, all further experimental results and graphs presented in this report will specifically pertain to this sensor module.

Our work was based on conducting series of experiments and obtaining some data. To carry out the experiment, we used a system that consists of several components. The key elements are high voltage supply, power supply for the board, X-ray tube, high voltage board (Figure 5) and of course the detector.

Figure 5: Experimental setup components (The high voltage supply (top left); the power supply for the board (top right); the X-ray tube (bottom left); the high voltage board (bottom right))

The high voltage supply allowed us to adjust the voltage on the HV board and accordingly on the detector within a range from 0 to -1000 volts. This was done during the experiment in steps of either 100 volts or 50 volts, depending on the number of data points we aimed to obtain for constructing the final graph and conducting further analysis. Using the Mini-X X-Ray Tube, we generated an X-ray beam, which was detected by the detector. Different types of experiments conducted using this system, as well as the results that can be derived from them will be discussed later.

During the experiments, several parameters could be varied, specifically the acquisition time, gain (high/medium/variable), voltage on the detector (from -100V to -1000V), signal frequency, power of the X-ray tube, as well as the number of memory cells (memory cells in AGIPD detectors store the charge collected from each X-ray pulse). However, in most experiments, some parameters were kept constant. Specifically, the number of memory cells was set to one, the frequency was 4.5 MHz, and the power of the X-Ray Tube was 3000 mW.

4 Results and Discussion

4.1 Mechanical assembly

During the course of our work, we were unable to test all the detectors, specifically those made from Gallium Arsenide, and Cadmium Telluride. We couldn't test them because only one of the

detectors, the Cadmium Zinc Telluride (CZT), was ready for testing. A photo of this module is presented in the Figure 6.

Figure 6: Cadmium Zinc Telluride module

Due to the detector's high sensitivity to environmental changes and its fragility, we decided to design a protective cover to shield our module from scratches, chips, and other mechanical damages (Figure 7).

(a) 3D model of the cover

(b) The module with the cover

Figure 7: Protection cover

Therefore, we adapted and 3D printed a special protective cover that can be mounted directly onto the copper interposer. The cover is secured using screws, which significantly enhances the safety and ease of handling and transporting the module. However, when operating the X-ray tube, it is necessary to remove this cover.

Additionally, the entire experiment is conducted in an X-ray protected, enclosed room, which ensures that no X-rays can escape when the X-ray source is active. This safety measure is crucial for protecting the surrounding environment and personnel from radiation exposure during the experiment.

4.2 Pulse Capacitor Scan

A Pulse Capacitor scan (PC scan) refers to a calibration process used to optimize the performance of the detector. PC scan routines helps to understand the behavior of AGIPD's pixel electronics and evaluate gain adjustment configurations. The first step is to inject charges of the AGIPD pixel electronics (preamplifier, integrator and capacitors that control the gain). The resulting curve exhibits how these components interact when varying amounts of charge are injected, simulating the effects of incoming X-ray photons.

During the experiment, we acquired three scans of the CdZnTe Quad Sensor, corresponding to high, medium, and variable gain settings. These scans were performed under controlled conditions,

with several key parameters held constant: the number of memory cells was set to one, the acquisition time was fixed at 12 clock cycles, and the signal frequency was kept at 4.5 MHz. The first image of this scan, corresponding to no injected charges, is illustrated in the Figure 8, where the chosen pixels are also highlighted.

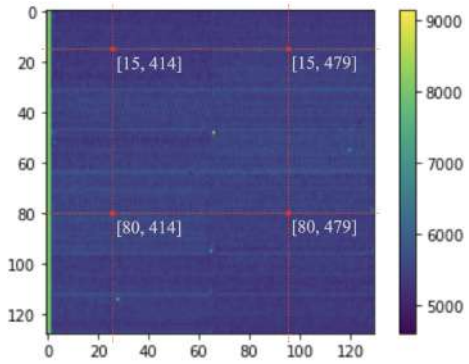

Figure 8: Dark image of four ASICs (64x64 pixels each), markers are pointing at the pixels that were chosen for the plots

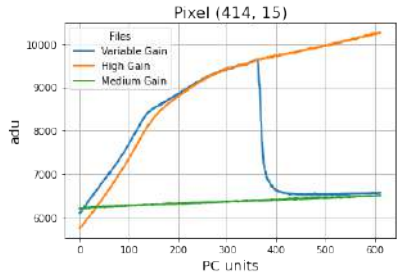

(a) Pulse capacitor scan for pixel 414,15

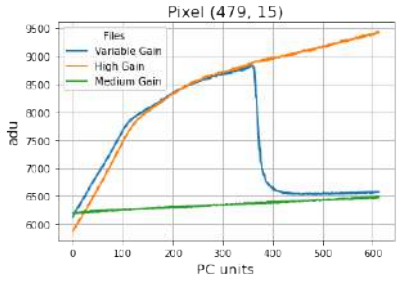

(b) Pulse capacitor scan for pixel 479,15

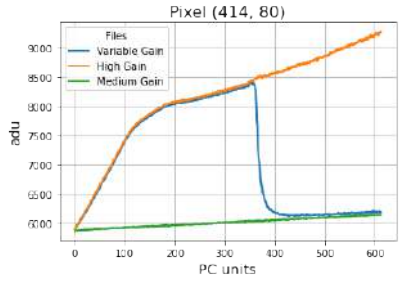

(c) Pulse capacitor scan for pixel 414,80

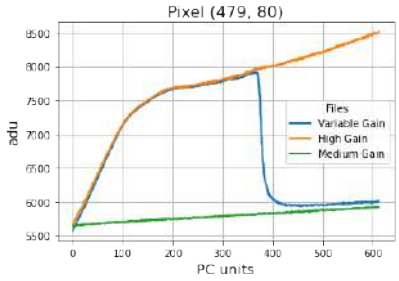

(d) Pulse capacitor scan for pixel 479,80

Figure 9: Pulse capacitor scan for four different pixels from each ASIC

Following the scans, we generated characteristic curves for selected pixels ([414,15], [479,15],

[414,80], [479,80]) from each ASIC on the sensor (Figure 9), allowing for a detailed analysis of their performance under the different gain settings.

However the provided graphs reveal issues with the pulse capacitor scans of the CdZnTe Quad Sensor, specifically with delayed gain switching. Ideally, the transition from High Gain to Medium Gain we should see around 9000 adu, when the response of the detector starts to be non-linear, but it occurs at 9500 adu. As a result, we have non-linear responses, which leads to complicated calibration and reduced accuracy.

Two main factors could be causing this problem. Either the threshold configuration of the chip is not optimized, delaying the switching; or the dark signal is too high, reducing the dynamic range of the high gain.

Further investigation is required to pinpoint the exact cause, whether it's due to the electronics or the material properties. Addressing this issue is essential for ensuring the detector's accurate performance in X-ray experiments.

4.3 Current vs. Voltage behaviour

The current-voltage (I-V) characteristic curve obtained from testing the CdZnTe Quad Sensor, where the voltage was varied from 0V to -1000V and back in 50V steps, provides valuable insights into the sensor's leakage current behavior (Figure 10).

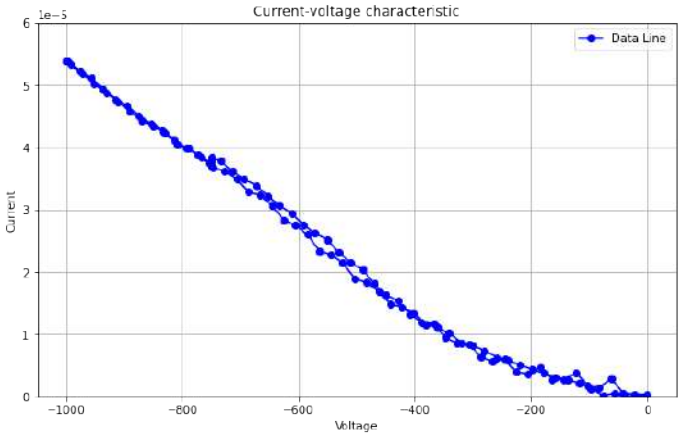

Figure 10: Current vs Voltage Response of the CZT quad sensor

The curve displays a generally increasing current with increasing negative voltage, which is typical of reverse-biased semiconductor materials. This behavior suggests that the sensor is functioning as expected, with the current gradually increasing as the applied voltage becomes more negative.

However, when calculating the leakage current, a significant discrepancy was observed. The expected leakage current was around 0.2 nA/mm^2, but the measured value for the entire sensor area was approximately 66 nA/mm^2. This difference is quite substantial and indicates that the actual leakage current is far higher than anticipated. Such a deviation calls for further investigation to identify the underlying causes.

At higher negative voltages, the response appears nearly linear, indicating a stable operation without significant non-linear effects. This stability is crucial for ensuring the sensor's reliability

in detecting X-ray signals. However, any deviations from this linearity or any hysteresis observed between the upward and downward voltage sweeps might indicate the presence of charge trapping or saturation effects within the material (CdZnTe in this case). Such hysteresis could reveal that the leakage current is influenced not only by the instantaneous voltage but also by the previous voltage history, pointing to possible non-idealities in the sensor's behavior.

4.4 X-ray Images

In our research, we conducted a series of three experiments, with the final one involving the use of an activated X-Ray beam. Initially, we performed a procedure known as a Dark Scan, where the X-Ray source is turned off. This scan was conducted by varying the voltage across a range from -100 volts to -1000 volts in increments of -50 volts, allowing us to capture a baseline signal unaffected by the X-Ray beam, for each bias voltage step (Figure 11 a).

After completing the Dark Scan, we activated the X-Ray source, specifically the Mini-X X-Ray Tube, and focused the beam onto the detector. We then conducted a series of measurements over the same voltage range, capturing images under the influence of the X-Ray beam. Subsequently, we selected a specific region on the detector, located at the center of the X-Ray beam, which consisted of a 20 by 20 pixel area, totaling 400 pixels (Figure 11 b).

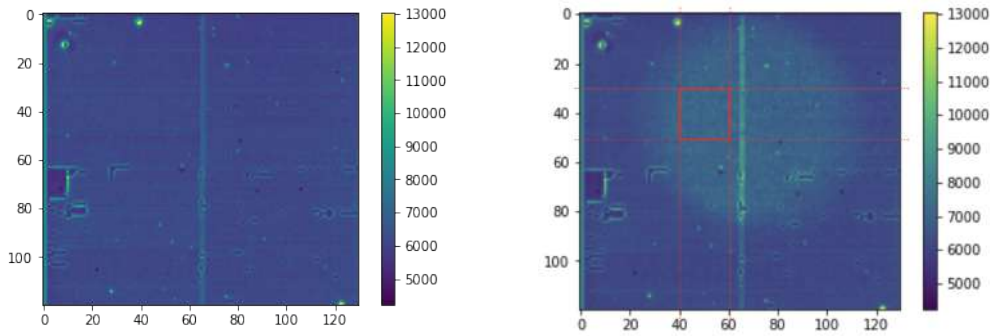

(a) Dark scan (b) X-rays scan

Figure 11: Scans

For each pixel within this area, we plotted a characteristic curve to show the pixel's response to varying voltage levels during both the Dark Scan and the X-Ray Scan (Figure 12).

To isolate the signal specifically caused by the X-Ray beam, we subtracted the Dark Scan data from the X-Ray Scan data, resulting in what we referred to as the isolated beam intensity signal. By averaging this signal across all 400 pixels, we generated a final curve that represents the overall response of the detector to the X-Ray beam across the voltage range.

A critical observation can be seen in Figure 13, where at a certain point, the sensor appeared to reach a depletion state but later the signal continued to rise. This suggests that the sensor had not fully depleted. A plausible explanation for this behavior could be a high level of leakage current, which might obscure the true depletion level, preventing the curve from accurately reflecting the point at which the sensor is fully depleted. As a result, the signal continues to increase beyond the expected depletion voltage, complicating the interpretation of the sensor's response under these conditions.

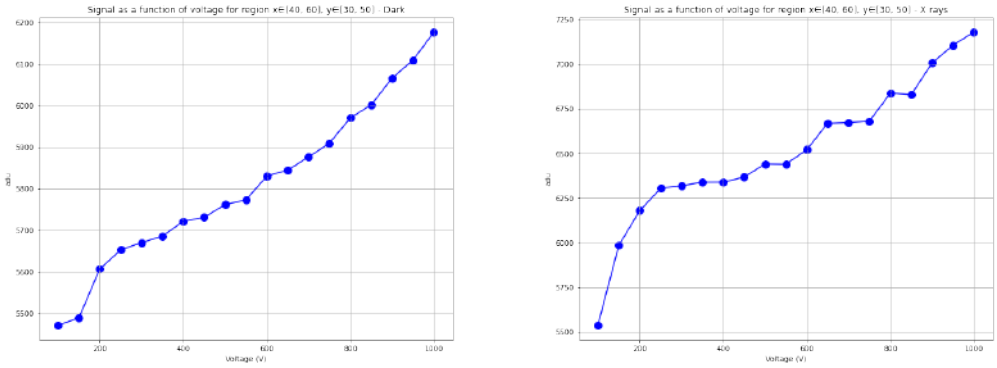

(a) Counts as a function of bias voltage for dark scan

(b) Counts as a function of bias voltage for X-ray scan

Figure 12: Signal as a function of bias voltage for both scans (high gain) for previously chosen area

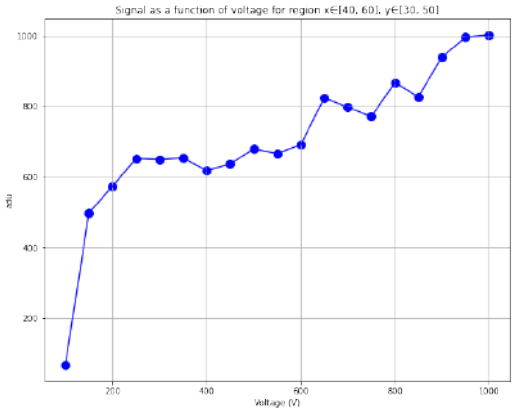

Figure 13: Isolated X-Ray beam signal as a function of the Bias voltage

5 Conclusion and Future Prospects

During the course of this work, we made significant progress in evaluating the performance of high-Z AGIPD detector prototypes, with a particular focus on the CdZnTe quad sensor. However, several challenges emerged that require further attention. One of the key difficulties we encountered was the relatively high leakage current. The expected value of the leakage current was approximately 0.2 nA/mm^2, but our measurements showed a much higher value of around 66 nA/mm^2. This large discrepancy indicates the need for further investigation into the sensor's material properties and the overall configuration of the system.

Additionally, the threshold settings revealed that the system is not yet fully optimized. Delays in gain switching and non-linearities in the response were observed, complicating the calibration process. Adjustment of the system parameters are required.

Finally, we observed that the sensor did not reach full depletion at the expected voltage during X-ray beam experiments. This behavior, likely influenced by the high leakage current, indicates

that the sensor's response under certain operating conditions still needs refinement.

To address these challenges, future efforts will focus on optimizing the threshold and gain settings, conducting tests with the X-ray source at different temperatures, and investigating the causes of the high leakage current. Upcoming beamtime at the High Energy Density (HED) facility in November 2024 will be crucial for characterizing the sensor's performance, particularly regarding afterglow effects and high-flux response, providing deeper insights into the viability of high-Z AGIPD detectors for high-energy applications.

References

[1] Helmuth Spieler. Pulse processing and analysis. http://www.physics.lbl.gov/ spieler, 2002. IEEE NPSS Short Course on Radiation Detection and Measurement.

[2] Ashkchan Allaghloobi, Julian Becker, Annette Delfs, Roberto Dinapoli, and et al. The adaptive gain integrating pixel detector at the european xfel. *Journal of Synchrotron Radiation*, 26:74–81, 2018.

[3] David Pennicard, Benoît Pirard, Oleg Tolbanov, and Krzysztof Iniewski. Semiconductor materials for x-ray detectors. *MRS Bulletin*, 42(6):445–450, 2017.

[4] B. Thomas, M.C. Veale, M.D. Wilson, P. Seller, A. Schneider, and K. Iniewski. Characterisation of redlen high-flux cdznte. *Journal of Instrumentation*, 12:C12045, 2017.

[5] M.C. Veale, C. Angelsen, P. Booker, and et al. Cadmium zinc telluride pixel detectors for high-intensity x-ray imaging at free electron lasers. *Journal of Physics D: Applied Physics*, 52:085106, 2018.

[6] D. Pennicard and H. Graafsma. Simulated performance of high-z detectors with medipix3 readout. *Journal of Instrumentation*, 6:P06007, 2011.